eureka Research article

Characterizing Lithium-Mediated Nucleoside Transport by Human Concentrative Nucleoside Transporters 1 and 3 (hCNT1 and hCNT3)

Received: 19 November 2021
Accepted: 26 February 2022
Published: 30 April 2022

Bhavana Kanagala[1*]
[1] Faculty of Science – Biological Sciences, University of Alberta
* Corresponding author: kanagala@ualberta.ca

ABSTRACT

The human concentrative nucleoside transporters (hCNTs) utilize coupling and movement of cations down their electrochemical gradient to mediate inward transport of nucleosides against their concentration gradient. Of the three hCNT family members, hCNT3 exhibits the broadest nucleoside selectivity and cation specificity, utilizing Na^+, Li^+, and H^+ to drive nucleoside transport. Xenopus laevis oocytes were injected with hCNT1 and hCNT3 RNA transcripts and incubated for 48 hours to allow protein expression and localization to the plasma membrane. The two-electrode voltage clamp (TEVC) method was used to perform electrophysiological studies. Oocytes were voltage-clamped, and currents were measured in response to various cation conditions, addition of different nucleosides and changes in membrane potential. Voltage-dependence of hCNT1- and hCNT3-mediated uridine uptake and hCNT3-mediated nucleoside uptake-induced currents was determined using NaCl, ChCl and LiCl transport media. Li^+ addition resulted in decreases in uptake of uridine both by hCNT1 and hCNT3. hCNT1 and hCNT3 exhibited similar trends in voltage-dependence of uridine transport; currents generated increased as potentials became more negative. It was shown that whereas Na^+-coupled hCNT3 has broad nucleoside selectivity, Li^+-coupled transport varied widely and was greatest for uridine, and least for thymidine (uridine > cytidine > guanosine > adenosine > inosine > thymidine). Our results indicate a possible role of the nucleoside nitrogenous base ring structure in the differential uptake of various nucleosides. Despite no significant role of Li^+ in vivo, further understanding of hCNT3 interactions with this cation may lead to a better understanding its transport mechanism and assist in the future design and delivery of effective anti-cancer drugs and anti-viral nucleoside drugs..

KEY WORDS: **electrophysiology, nucleoside transport, Xenopus laevis, two-electrode voltage clamp, secondary active transporters, influx rates**

1 | INTRODUCTION

Physiological Nucleoside Transporters

Eukaryotic cells rely on the cell's replication, transcription, and translation of nucleic acids to survive. Pyrimidine and purine nucleosides are converted into nucleotides which are required in many processes in eukaryotic cells, including nucleic acid synthesis and intermediary metabolism (King et al., 2006). Given the hydrophilic nature of nucleosides, their transport across plasma and organelle membranes and their cellular availability is dependent upon nucleoside transporters (NTs). NTs are also crucial in the therapeutic actions of purine and pyrimidine analogue anticancer and antiviral nucleoside drugs such as gemcitabine and zidovudine (Zhang et al., 2007, Patejko et al., 2018). Two classes of NTs were identified in mammals using radiolabeled nucleoside uptake studies: the concentrative nucleoside transporters, known in humans as SLC28 and equilibrative nucleoside transporters, known in humans as SLC29 (King et al., 2006; Zhang et al., 2007). Concentrative nucleoside transporters rely on cation electrochemical gradients across the plasma membrane to drive nucleoside influx into cells (King et al., 2006).

Cation Coupling Characteristics of hCNTs

The human concentrative nucleoside transporter (hCNT) family has three members, hCNT1, hCNT2 and hCNT3 (Smith et al., 2007; Smith et al., 2005; Yao et al., 2018; Young et al., 2013). All three hCNTs are secondary active inwardly directed transporters; they are also dependent on cation coupling to mediate nucleoside transport into the cell (**Figure 1**). hCNT1 and hCNT2 utilize the Na^{++} electrochemical gradient across the membrane, while hCNT3 uses Na^+ and H^+ gradients (Smith et al., 2005). The Na^+:nucleoside coupling ratio for hCNT3 is 2:1, and the corresponding H^+:nucleoside coupling ratio is 1:1 (Smith et al., 2007). Additionally, hCNT3 also utilizes the transmembrane electrochemical gradient of Li^+ to transport nucleosides (Smith et al., 2005). In contrast to largely Na^+-specific hCNT1 and hCNT2, hCNT3 exhibits dependence on Na^+, H^+ and Li^+, all of which are cations that support influx of nucleosides. The order of substrate binding to hCNT3 was elucidated by Smith et al. in which they showed that the cation binds to the transporter first, increasing the affinity of hCNT3 for the nucleoside, which binds second (Smith et al., 2005). Besides cation specificity, the three hCNTs also differ in their selectivity for nucleosides. While hCNT1 transports pyrimidine nucleosides and one purine nucleoside (adenosine), hCNT2 transports purine nucleosides and one pyrimidine nucleoside (uridine). Unlike hCNT1 and hCNT2, hCNT3 has a broader specificity as it is capable of transporting both pyrimidine and purine nucleosides using Na^+ gradients at similar levels (Young et al., 2013).

Structural Features of hCNTs

Substituted cysteine accessibility method (SCAM) analysis utilizes the reaction that occurs between cysteine residues and sulfhydryl reagents to localize specific residues within the transporter (Zhu et al., 2007, **Figure 1**). Mutation of endogenous cysteines in hCNT3 to serine generated a functional cysteine-less mutant (Mulinta et al., 2017). The crystal structure of a bacterial member of the concentrative nucleoside transporter family, Vibiro cholerae CNT (vcCNT), has also provided information on the structure of hCNT3. vcCNT has a relatively high sequence identity with hCNT1 and hCNT3 at 36% and 39%, respectively (Johnson et al., 2012). Recently, a cryogenic electron microscopy (CryoEM) structure of hCNT3 was determined at a resolution of 3.4 Å (Zhou et al., 2020). Uridine binding was not detected in hCNT3 under Na^+-free conditions, further indicating that Na^+ binding is required to form the nucleoside binding pocket of CNTs (Smith et al., 2005; Zhou et al., 2020). The CryoEM study, along with previous hCNT3 biochemical and structural investigations of bacterial CNTs reveals a common trimeric membrane architecture (Stecula et al., 2017; Johnson et al., 2012).

Hypothesis

The ability of hCNT3 to utilize Li^+ ions to transport nucleosides has been reported in a previous study (Smith et al., 2005, Gorraitz et al., 2010). The present study aims to characterize the kinetics of Li^+-dependent nucleoside transport in both hCNT1 and hCNT3. The voltage-dependence of both hCNT1 and hCNT3 transport in Li^+ will be compared to Na^+ by analyzing current-voltage (I-V) relationships. Given that the Li^+ ion is intermediate in size between Na^+ and H^+, it is hypothesized that hCNT1- and hCNT3-mediated transport in Li^+-containing medium will exhibit characteristics different from Na^+- (hCNT1 and hCNT3) and H^+- (hCNT3) containing transport media. Previous data have illustrated that nucleosides are transported by hCNT3 in Li^+ media with intermediate selectivity. Relative to current produced by uridine transport by hCNT3 in Li^+ media, the other nucleosides tested produced lower amounts of current during their transport (Young Laboratory, unpublished data). I hypothesize that I-V relationships for each nucleoside will mimic these patterns in maximum current (Imax) generated under voltage-clamped conditions.

2 | METHODS

Heterologous Expression in Xenopus laevis Oocytes

Female African clawed frogs, Xenopus laevis, were anaesthetized in a bath filled with 0.2% (w/v) tricaine methanesulfonate solution and then humanely euthanized following the guidelines of the Canadian Council on Animal Care. Oocytes extracted from euthanized X. laevis were treated with collagenase (2 mg/ml) for 2 hours. To remove follicular layers of the oocytes, they were treated with phosphate and manually defolliculated. After a minimum of 24 hours following defolliculation, oocytes were injected with either 10 nL of water containing 10 ng of hCNT1 or hCNT3 RNA transcript, or 10 nL of water alone (control group). To promote proper protein production and trafficking to the plasma membrane, oocytes were incubated for at least 48 hours before experimentation. Oocytes were incubated and stored at 17oC in modified Barth's medium (MBM; 88 mM NaCl, 1 mM KCl, 0.33 mM Ca(NO3)2, 0.41 mM CaCl2, 0.82 mM MgSO4, 2.4 mM NaHCO3, 10 mM Hepes, 2.5 mM sodium pyruvate, 0.1 mg/ml penicillin, and 0.05 mg/ml gentamycin sulfate, pH 7.5). MBM was changed daily to promote the health and survival of the oocytes.

Transport Media

Electrophysiological experiments were carried out in transport medium containing either Na+, H+ or Li+ ions. Na+ transport medium contained: 100 mM NaCl, 2 mM KCl, 1 mM CaCl2, 1 mM MgCl2, and 10 mM Hepes (pH 8.5). H+-mediated currents were studied using Na+-free, choline-containing transport medium, which was made using: 100 mM ChCl, 2 mM KCl, 1 mM CaCl2, 1 mM MgCl2. Li+ transport medium contained: 100 mM LiCl, 2 mM KCl, 1 mM CaCl2, 1 mM MgCl2 and 10 mM Hepes (pH 8.5). These solutions were made at either pH 5.5 (10 mM Mes) or pH 8.5 (10 mM Hepes). All solutions were refrigerated overnight and heated to room temperature by submersion in warm water. All reagents were purchased from Sigma-Aldrich (St. Louis, MO, USA) and Fischer Scientific (Waltham, MA, USA).

Nucleoside Solutions

Purine and pyrimidine nucleoside stock solutions were made either in 100 mM Na+ transport medium (uridine only) or 100 mM Li+ transport medium (uridine, adenosine, cytidine, guanosine, inosine and thymidine). All nucleoside stock solutions were made in their respective media at a concentration of 25 mM, except guanosine which was made at a concentration of 5 mM due to its inability to fully dissolve beyond this concentration. Stock solutions were diluted at specific dilution factors to a final concentration of 100 μM in the appropriate transport media

Two-electrode Voltage Clamp (TEVC)

Nucleoside-induced membrane currents in the oocytes were measured at room temperature (21 oC) using the Axoclamp 900A oocyte clamp (Molecular Devices, Inc.). The Axoclamp 900A, a computer-controlled microelectrode amplifier, was connected to a compatible computer using the Digidata 1440A A/C converter and the Tektronix DPO 2022B Digita Phosphor Oscilloscope. Current signals were filtered at 10 Hz and were sampled at 20 milliseconds. The glass microelectrodes were filled with a 3M KCl solution, facilitating an acceptable resistance range of 0.5 - 2.0 megaohms. Oocytes were penetrated with two glass microelectrodes, and any oocytes with unstable membrane potentials or resting membrane potentials more positive than -25 mV were not used. Oocytes were voltage-clamped at a holding potential (Vh) of -50 mV and currents (nA) were measured following changes to the cation, nucleoside or holding potential.

Cation-specificity of hCNT1 and hCNT3 Transport

Oocytes were voltage clamped at a holding potential (Vh) of -50 mV. Following the addition of 100 μM uridine in medium containing 100 mM NaCl (pH 8.5), 100 mM ChCl (pH 8.5), 100 mM ChCl (pH 5.5) or 100 mM LiCl (pH 8.5), inward currents were measured in hCNT1- and hCNT3-producing oocytes. Nucleoside (uridine)-induced currents in Na+, H+ or Li+ were consecutively measured on the same oocyte. The experiment was repeated on 7 hCNT1- and hCNT3- expressing oocytes in addition to water (H2O)-injected oocytes. Currents are shown in the form of a bar graph as the mean inward current (nA) ± standard error of the mean (SEM) for each experimental condition. No currents were induced by uridine in control water-injected oocytes, indicating the transporter-dependent nature of the induced currents.

Current-Voltage (I-V) Curves

Oocytes were voltage-clamped at a holding potential (Vh) of -50 mV. Currents were generated using transport media alone (100 mM NaCl (pH 8.5), 100 mM ChCl (pH 5.5) or 100 mM LiCl (pH 8.5)), and then with 100 μM uridine in the appropriate transport media. 100 mM NaCl contained Na+ cations only, 100 mM ChCl (pH 5.5) contained H+ ions only and 100 mM LiCl contained Li+ cations only. The difference between steady-state currents invoked in the presence and absence of uridine during 300-millisecond voltage pulses to potentials between +60 mV and -110 mV were used to generate current-voltage (I-V) curves and compare the voltage-dependence of the different cations (Na+, H+, and Li+). In addition to uridine-induced I-V curves (hCNT1 and hCNT3), 5 other nucleosides (adenosine, cytidine, guanosine, inosine and thymidine; hCNT3) were tested to determine the I-V relationships of nucleoside transport in Li+-containing media.

Statistical Analysis

An unpaired t-test was performed to determine statistical significance of the results. p-values were calculated with respect to changes in current compared to current resulting from transport media alone, with $p < 0.05$ considered as statistically significant. Absolute values of current measurements (nA) at each voltage potential step in hCNT1 and hCNT3 oocytes were used in calculations. The same process was used in statistical calculations of the currents elicited in control (water-injected) oocytes. Currents are represented as mean values from 10 replicate experiments with hCNT1/hCNT3-injected oocytes and 4 replicate experiments with water-injected oocytes ± standard error.

3 | RESULTS

Uridine-induced Currents Mediated by hCNT1 and hCNT3

hCNT1 mediates inward transport of nucleosides coupled to the symport of 1 Na^+ from the extracellular space into the cell cytoplasm. On the other hand, hCNT3 utilizes 2 Na^+ or 1 H^+ cations to transport nucleosides into the cell. The resulting inward current was measured using a two-electrode voltage clamp (TEVC) to hold the plasma membrane potential (Vm) at a desired command voltage (Vcmd), which is -50 mV for our experiments. The amplifier measures the difference between Vm and Vcmd and then generates currents in response to changes in Vm to maintain Vm at the pre-established Vcmd. While transport occurs, the current injected into the oocyte is recorded, with inward currents displayed as a downward deflection and an outward current displayed as an upward deflection in the traces. Both hCNT1 and hCNT3 utilize Na^+ cations for transport of nucleosides into the cell, and exhibited current traces that showed downward deflections, indicating inward current in Na^+-containing transport medium (100 mM NaCl, pH 8.5). Since

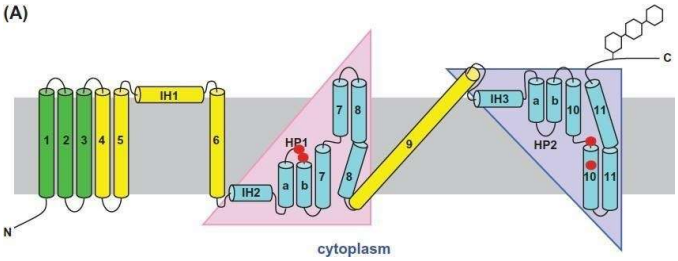

Figure 1. Topological model of hCNT3. Predicted membrane topology of hCNT3 based on the structure and topology of vcCNT from Vibiro cholera, which is a bacterial counterpart of hCNT3. Like vcCNT and CNTNW, hCNT3 exhibits intracellular N termini and extracellular C termini. TM9 in yellow represents the scaffold domain of hCNT3, a critical component of the elevator mechanism and transport function of hCNT3. Red circles indicate residues Gln341, Thr342, Asn565 and Ile571 which are sensitive to PCMBS inhibition and uridine protected (11).

hCNT1 does not couple nucleoside transport with H^+ ions, minimal inward currents were generated in Na^+-free, acidified choline-containing conditions (100 mM ChCl, pH 5.5 and 8.5) (**Figure 2**). hCNT1 also exhibited inward currents in Li^+-containing media. Given the greater 2:1 Na^+:nucleoside coupling ratio of hCNT3 compared to hCNT1, hCNT3 exhibited larger inward currents during transport in Na^+-containing conditions (100 mM NaCl, pH 8.5). hCNT3 exhibited increased inward currents in response to increasing concentrations of H^+ in Na^+-free transport media (100 mM ChCl pH 8.5 vs pH 5.5). hCNT3 also generated uridine-induced Li^+ currents which were slightly smaller than H^+ currents. Lastly, minimal to no inward currents were observed in control-water oocytes in any of the four different transport media as they do not possess hCNT transporters. Mean currents generated under the different conditions are summarized in **Figure 2**.

Effects of Li^+ on hCNT1 and hCNT3 Uridine-Induced Currents

Li^+-coupled nucleoside transport was measured in the presence of Na^+ to reveal the effects of Li^+ on maximal Na^+-mediated uridine transport by hCNT1 and hCNT3 (**Figure 3**). Uridine-induced current was measured in Na^+-containing, Li^+-free transport medium (95 mM NaCl and 5 mM ChCl, pH 8.5) and then in Na^+- and Li^+-containing transport media (95 mM NaCl and 5 mM LiCl, pH 8.5). Based upon a similar study of the

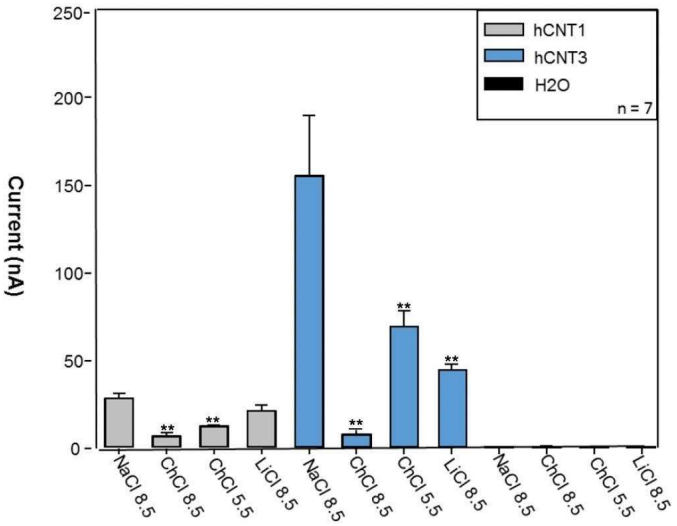

Figure 2. Uridine-induced currents in hCNT1-, hCNT3- and H2O-injected oocytes in the presence of Na^+, H^+ and Li^+. Inward currents were measured in the presence of Na^+ (100 mM NaCl, pH 8.5), H^+ (100 mM ChCl, pH 5.5), Li^+ (100 mM LiCl, pH 8.5) or in the absence of Na^+, H^+ and Li^+ (100 mM ChCl, pH 8.5). 100 μM uridine was added to the transport media. Grey and blue bars represent current mediated by hCNT1 and hCNT3, respectively, while black bars represent current from H2O-injected oocytes (control group). Compared to Na^+-coupled transport in hCNT1 oocytes, transport in the absence of Na^+, H^+ and Li^+ (100 mM ChCl, pH 8.5) resulted in a 72% decrease in current ($p = 0.013$) while H^+-coupled transport resulted in a 54% decrease ($p = 0.029$). Compared to Na^+-coupled transport in hCNT3 oocytes, transport in the absence of Na^+, H^+ and Li^+ (100 mM ChCl, pH 8.5) resulted in a 91% decrease while H^+-coupled transport resulted in a 55% decrease ($p = 0.022$) and Li^+-coupled transport resulted in a 68% decrease in current ($p = 0.019$). In the control group with no cell surface hCNT1/3 expression, no significant current was generated.

Na^+/dicarboxylate cotransporter (NaDC-1) (7), we expected to see lower inward current in the presence of Na^+ and Li^+ compared to Na^+ alone in both hCNT1 and hCNT3. In our results, we found that the presence of Li^+ does indeed reduce the inward uridine-induced Na^+ current generated in both hCNT1 and hCNT3. In hCNT1, despite a 31% decrease in uridine-induced current in the presence of both Li^+ and Na^+ ions compared to Na^+ alone, the reduction was not statistically significant. In hCNT3, transport of uridine in the presence of both Li^+ and Na^+ ions resulted in a

reduction of 43% in the uridine-induced current in the presence of Na^+ alone, which was statistically significant. Lastly, we did not observe any detectable levels of inward current in the control water-injected group.

Current-Voltage (I-V) Relationship of Uridine Transport

Analysis of I-V relationships of hCNT1 and hCNT3 transport currents helped reveal the effects of membrane potential (Vm) on nucleoside-induced steady-state currents. Similar to a previous study on hCNT3, uridine-induced currents in the presence of Na^+ or H^+ at potentials between -110 mV and +60 were shown to be voltage-dependent and increased in magnitude as the membrane potential became more negative (Smith et al., 2005).

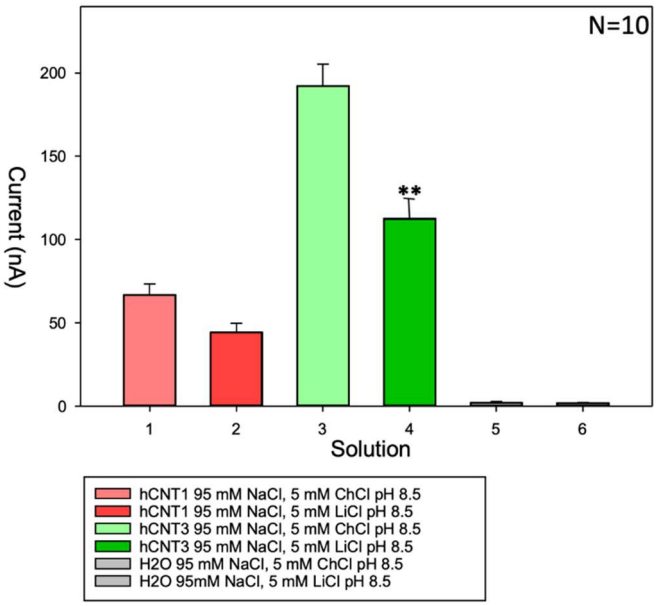

Figure 3. Uridine-induced current in hCNT1-, hCNT3-, and water-injected oocytes in the absence or presence of Li^+ ions in NaCl solution. Inward currents were measured with 100 μM uridine in the presence of Na^+ ions only (95 mM NaCl and 5 mM ChCl, pH 8.5) or in the presence of both Na^+ and Li^+ ions (95 mM NaCl and 5 mM LiCl, pH 8.5). The red bars represent hCNT1-mediated uridine-induced currents and the green bars represent hCNT3-mediated uridine-induced currents. The grey bars represent water-injected oocytes (control group). Compared to Na^+-coupled transport mediated by hCNT1, the addition of 5 mM Li^+ resulted in a 31% decrease in current. Compared to Na^+-coupled transport mediated by hCNT3, the addition of 5 mM Li^+ resulted in a 43% decrease in current ($p = 0.015$). In the control group with no cell surface hCNT1/3 expression, no significant current was generated.

Voltage-dependence of hCNT1 and hCNT3 transport under various cation conditions was examined by generating I-V curves (**Figure 4**). The difference between steady-state currents recorded in the presence and absence of 100 μM uridine in Na^+-containing (100 mM NaCl, pH 8.5), Na^+-free, H^+-containing (100 mM ChCl, pH 5.5) and Na^+- and H^+-free, Li^+-containing (100 mM LiCl, pH 8.5) transport media was examined. Currents generated in hCNT1 and hCNT3 following the application of uridine demonstrated voltage-dependence among all three cations (Na^+, H^+ and Li^+) (**Figures 4a and 4b**). hCNT1 and hCNT3 showed similar trends in voltage-dependence during uridine uptake; both transporters exhibited larger inward currents at more negative potentials and non-linear decreases in current as potentials became more positive (**Figures 4a and 4b**). As potentials approached +60 mV, currents mediated by hCNT1 and hCNT3 approached but did not exceed 0 nA (**Figures 4a and 4b**).

Despite this similarity, the magnitude of current generated by uridine uptake under the three cation conditions differed between hCNT1 and hCNT3. hCNT3 exhibited larger currents than hCNT1 with all three cations tested (Na^+, H^+ and Li^+). However, in both hCNT1 and hCNT3 at all potentials examined, currents were the largest in the presence of Na^+ and lowest in the H^+. Currents in the presence of Li^+ were intermediate to Na^+ and H^+ (**Figures 4a and 4b**). Water-injected oocytes did not exhibit any detectable levels of uridine uptake, evidenced by the current ranging from +4 to -4 nA (**Figure 4c**).

Use of I-V Curves to Determine Substrate Selectivity of hCNT3 in Li^+

It has been established that nucleoside transport mediated by hCNT3 differs depending on the driving cation (Smith et al., 2005). Studies from the Young laboratory demonstrated varying levels of nucleoside transport depending on the cation used, with Na^+ being the most permissive, H^+ the most restrictive and Li^+ exhibiting intermediate results (Smith et al., 2005, unpublished data). In light of the differences found between Na^+- and H^+-coupled transport compared to Li^+-coupled transport, we analyzed in detail the substrate selectivity of hCNT3 in the presence of Li^+ looking at the I-V relationship (**Figure 5**). The voltage-dependence of transport and differences in current magnitudes generated with different pyrimidine and purine nucleosides are shown. The results indicate that uridine-induced currents were significantly greater in Na^+- than in Li^+-containing medium (**Figure 5a**). Currents generated by the nucleosides in Li^+-containing medium were from highest to lowest: uridine > cytidine > guanosine > adenosine > inosine > thymidine. Guanosine is transported in Li^+-containing media, however the current generated by guanosine transport is lower than that of uridine and cytidine, both of which are pyrimidine nucleosides (**Figure 5a**). Thymidine transport in Li^+-media with currents increasing as the membrane potential became more negative. These results are consistent with previous experiments looking at substrate selectivity where hCNT3-injected oocytes

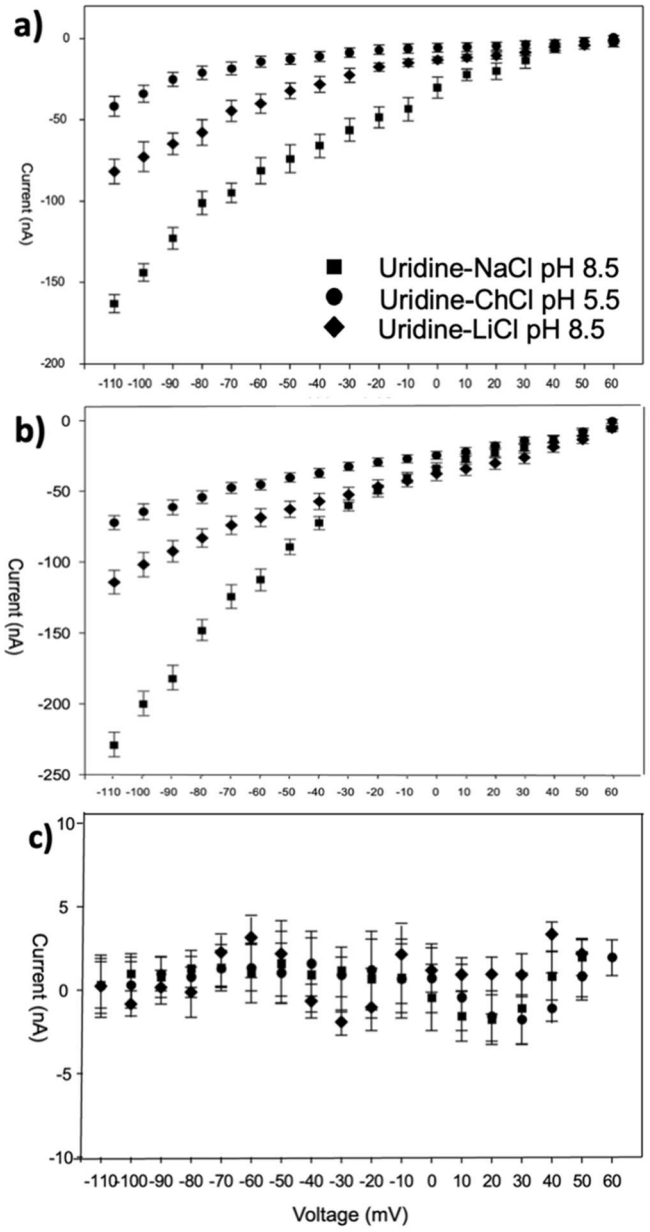

Figure 4. Voltage-dependence of uridine transport-induced currents mediated by hCNT1-, hCNT3- and water-injected oocytes. Voltage pulses were given from a Vh of -50 mV to potentials wrangling from -110 mV and +60 mV, increasing in 10-mV steps. Current-voltage (I-V) curves for hCNT1, hCNT3- and water-injected was generated using the difference between steady state currents recorded in the presence and absence of 100 μM uridine in Na+-containing (squares), H+-containing (circles) and Li+-containing (diamonds) transport media. The data are represented the average of currents generated by 9 oocytes expressing hCNT1 and hCNT3 and 4 water-injected oocytes. a) Current-voltage (I-V) curves for hCNT1. b) Current-voltage (I-V) curves for hCNT3. c) Current-voltage (I-V) curves for water-injected oocytes. No uridine-induced currents were observed in the control, water-injected oocytes.

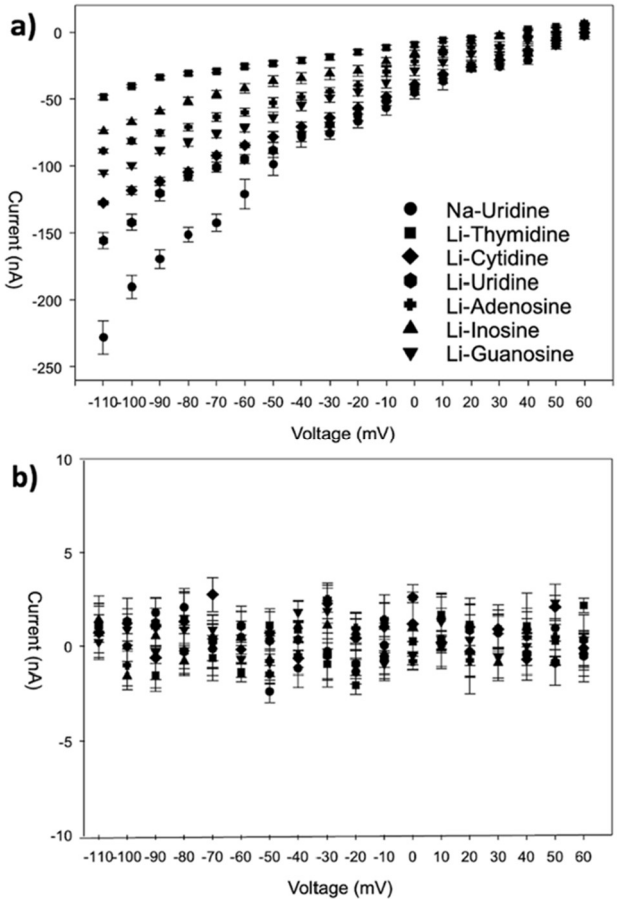

Figure 5. Voltage dependence of nucleoside transport-induced currents mediated by hCNT3- and water-injected oocytes. Voltage pulses were given from a Vh of -50 mV to potentials ranging from -110 mV and +60 mV, increasing in 10-mV steps. Current-voltage (I-V) curves for hCNT3- and water-injected oocytes were generated using the difference between steady state currents recorded in the presence and absence of 100 μM uridine in Na+-containing (circles) and Li+-containing (hexagon) solutions. Other nucleosides were examined in Li+-containing media only, including thymidine (squares) and cytidine (diamonds), adenosine (cross), inosine (upwards triangle) and guanosine (downwards triangle). The data are represented as an average of currents generated by 10 oocytes expressing hCNT3 and 4 water-injected oocytes. a) Current-voltage (I-V) curves for hCNT3. b) Current-voltage (I-V) curves for water-injected oocytes. No uridine-induced currents were observed in the control, water-injected oocytes.

were voltage-clamped at one potential only, -50 mV, and inward currents measured following the addition of pyrimidine and purine nucleosides in the presence of Li+. The same trend in current magnitude was observed in these experiments (Young laboratory, unpublished observations). In water-injected oocytes, no significant current was generated with any of the nucleosides examined (**Figure 5b**).

4 | DISCUSSION

The unique ability of hCNT3 to couple two Na+ ions with the import of one nucleoside (2:1 Na+:nucleoside coupling ratio) stems from the presence of two cation binding sites in the transporter while hCNT1/2 only possess one cation binding site, resulting in a 1:1 Na+:nucleoside coupling ratio exhibited by

these transporters. However, in the presence of H+ ions only, hCNT3 shifts to a 1:1 H+:nucleoside coupling ratio. This unique property of hCNT3 can be utilized pharmacologically to attain greater concentrations of nucleosides and nucleoside-analogue drugs import into the cell. The greater energy generated from the use of two Na+ ions can better overcome the challenges posed by greater concentrations of nucleosides (Smith et al., 2007).

The Effects of Li+ on Uridine-induced Currents of hCNT1 and hCNT3

The Na+/glucose transporter (SGLT1), the bacterial melibiose cotransporter (MelB) and the sodium dicarboxylate cotransporter (NaDC-1) all exhibit decreased inward currents in Na+-free, Li+-containing as well as Na+- and Li+-containing transport media compared to Na+-containing, Li+-free media (2, 7). Li+ binding likely results in an altered conformational change compared to changes that occur when Na+ binds to hCNT1 or Na+ and H+ bind to hCNT3. This altered conformation may result in impairment of consequent nucleoside binding to the transporter, thereby reducing nucleoside-mediated current; this could be a future avenue for investigation.

Despite the higher affinity of hCNT3 for H+, H+-uridine coupled transport was considerably lower than Na+-coupled transport. Also, despite reports of H+ supporting higher maximal rates of uridine and adenosine transport in hCNT3, the transporter efficiency was shown to be lower in H+ than in Na+ medium (17). Similar results were seen in NaDC-1 which exhibits a greater affinity for Li+; however, Li+ binding decreases succinate-induced currents compared to currents generated in Na+ (7). Taken together, these results indicate that the binding of H+ to hCNT3 may produce less favorable conditions for transport compared to binding with Na+. It has been established that hCNT1 does not mediate nucleoside transport in Na+-free, H+-containing conditions. Our results (**Figure 2**) agree with these findings as we observed minimal levels of uridine transport across hCNT1 in H+-containing, Na+-free conditions (ChCl pH 5.5), while hCNT3 showed detectable levels of uridine transport under the same conditions.

Pajor et al. (1998) demonstrated using the Na+/dicarboxylate cotransporter (NaDC-1) that the addition of Li+ ions to NaCl solution results in decreased uptake of succinate, as evidenced by a decrease in maximal current (Pajor et al., 1998). Given the cation coupling and inwardly directed characteristics of NaDC-1, we used these findings as a basis for investigating the role of Li+ in uridine-induced current with hCNT1 and hCNT3. We found that under identical conditions (100 μM uridine), the addition of 5 mM LiCl to 95 mM NaCl medium has inhibitory effects on the uptake of uridine. Similar to the NaDC-1 (Pajor et al., 1998), addition of Li+ did not result in statistically significant reductions in maximal current in hCNT1. However, hCNT3 exhibited statistically significant reduction in maximal current, indicating a lesser inhibition by Li+ on hCNT3 relative to the hCNT1 and NaDC-1 cotransporters (Pajor et al., 1998).

Current-voltage and Cation Dependence of Uridine Transport

Na+:nucleoside and H+:nucleoside I-V curves and the effect of Vm on current values indicated the influence of Vm on carrier translocation in hCNT proteins, since the driving force for hCNTs relies not only on the nucleoside and cation gradients, but also on the Vm. Despite all three cations supporting electrogenic uridine influx, hCNT1 and hCNT2 are largely Na+-specific while hCNT3 can cotransport Na+, H+, and Li+. Despite differences in the level of current generated by hCNT1 and hCNT3 in different cation conditions, transport of uridine by both transporters was electrogenic. Consistent with previous studies, hCNT1 and hCNT3 exhibited increased uridine transport at more negative potentials (Smith et al., 2004).

Based upon previous studies which showed that inward currents mediated by hCNT1 and hCNT3 increased as the Na+ cation concentration increased, it may have the same effect if the H+ concentration is increased (Smith et al., 2007). Smith et al. showed that nucleosides generated significantly higher levels of current in solutions with a pH of 5.5 compared to pH of 8.5 (Smith et al., 2005). This differential result is because solutions with a pH 5.5 contains proton concentration 1000 times higher than pH 8.5. Results in this study demonstrated cation dependence of transport with hCNT1 and hCNT3 (**Figures 2 and 4**).

Different cations bind to the primary cation binding site of hCNT proteins and induce different conformational changes based on their size. Given that Na+ is a different size compared to hydronium ions (the form of H+ which is coordinated by the cation binding pocket) and Li+ ions, it can interact differently with the residues involved in the primary cation binding site. This differential interaction by the cations may be why the hCNT proteins exhibit different levels of transport under certain conditions, however more research into the topic is required.

Substrate Selectivity of hCNT3

Despite broad nucleoside selectivity by hCNT3 in Na+, Smith et al. reported a different substrate selectivity profile in H+. In the presence of H+, currents were largest with uridine followed by thymidine, cytidine, adenosine, and inosine (Smith et al., 2005). Transport of guanosine by hCNT3 in H+ transport media was very low and pH-independent (Smith et al., 2005).

This change in the substrate selectivity profile of the transporter suggests that substrate specificity is dependent on the coupling cation and not an intrinsic characteristic of the transporter itself. Results in this study demonstrate differing current magnitudes (**Figures 2 and 4**) and substrate selectivities (**Figure 5**) for hCNT3 depending on the cation present.

Given the high selectivity of hCNT3 for uridine over other nucleosides in the presence of H^+ and Li^+ under the same experimental conditions, there must be a structural difference between uridine and the other nucleosides resulting in this preferential uptake of uridine. For example, uridine is the least bulky out of all the nucleosides used in this study, indicating that its smaller spatial size may lend to its preferential uptake by hCNT3 (**Figure 1**). Li^+ permitted a broad nucleoside selectivity by hCNT3, which is evidenced by the generation of detectable levels of current by all nucleosides examined (**Figure 5a**). It was interesting to find that uridine elicited the greatest current at all potentials while thymidine generated the least current across all potentials. Despite both nucleosides belonging to the pyrimidine family, they have major structural differences; thymidine lacks a hydroxyl group at the C2' position of the ribose sugar and has a methyl group at the C5 position of the nitrogenous base (**Figure 6**). While this may be the reason for drastic reductions in current mediated by thymidine uptake, more research is required to elucidate whether this is the case, and if it is, which of the two structural features are responsible for this phenomenon.

Inosine and adenosine presented with lower levels of current than cytidine and guanosine (**Figure 5a**). It was interesting to find that inosine and adenosine share structural similarities while cytidine and guanosine also share structural similarities. Despite belonging to different nucleoside subfamilies (cytidine is a pyrimidine while guanosine is a purine), these nucleosides possess two functional groups (primary amine (-NH2) and amide (-N=O)), both of which are the same in each nucleoside (**Figure 6**). In contrast, adenosine, and inosine, despite both belonging to the purines possess only one functional group attached to the nitrogenous base. It is worth noting that uridine also has two functional groups attached to the nitrogenous base while cytidine, which elicited the smallest current, has three functional groups. So, it may be that the presence of exactly two functional groups on the nitrogenous base may allow for more favourable coordination of nucleosides at the nucleoside binding site. The role of nucleoside structure on nucleoside uptake and resulting current under various cation conditions is also a possible future research avenue.

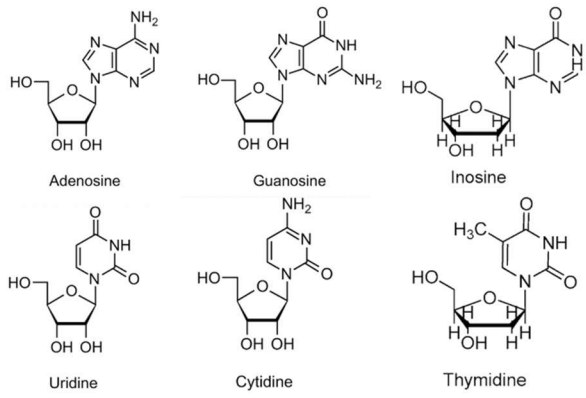

Figure 6. Structures of the physiological nucleosides transported by hCNT3. The nucleosides in the top panel are adenosine, guanosine, and inosine – all of which belong to the purine subfamily of nucleosides. The nucleosides in the bottom panel are uridine, cytidine, and thymidine – all of which belong to the pyrimidine subfamily of nucleosides. The nucleosides exhibit several structural differences from each other, even if belonging to the same subfamily, which may lead to altered binding at the substrate binding site in hCNT3. This can result in changes in current generation by the transport of each of these nucleosides by hCNT3. Images acquired from Patejko et al. (2018).

5 | LIMITATIONS AND FUTURE RESEARCH

Major limitations of our study were the time constraints brought on due to the covid-19 pandemic as well as the declining viability and quality of oocytes. As the year progressed, we saw a general decline in the stability of resting membrane potentials that the egg presented with. Li^+ cations are not available physiologically for utilization by hCNT1 and hCNT3 for nucleoside transport. Therefore, hCNT1 and hCNT3 cation specificity in Li^+-containing solutions may not be physiologically relevant. Another limitation of this study are issues associated with voltage-clamping the oocytes for an extended period and subjecting them to multiple conditions for the IV curve experiments; it is significantly taxing on the oocytes. Significantly lower levels of currents are observed following the addition of H^+ or Li^+ cations compared to Na^+; this was a limitation as even slight deviations in oocyte quality or resting membrane potential resulted in an inability to measure these low currents. A stable resting potential more negative than -25 mV is very important when performing I-V curve experiments however, many of the oocytes examined did not present this low of a potential and/or showed fluctuating potentials, making it difficult to acquire accurate current readings. Without a stable clamp, the baseline, or holding current of the oocyte drifts as IV experiments are in progress. When the baseline drifts, current traces in the presence and absence of substrate cannot be subtracted, meaning experimental results cannot be obtained from these oocytes. Lastly, the Xenopus oocytes require about 48 hours to fully

express the hCNT proteins upon injection RNA transcript, resulting in a delay of experiments.

Nevertheless, further studies of transport mediated by various cations via hCNT1 and hCNT3 will help better elucidate the functional characteristics of these transporters. While hCNT1 and hCNT3 do not perform Li^+-coupled nucleoside transport in vivo, characterizing Li^+ cation transport and corresponding nucleoside specificity will help in developing new anti-cancer and anti-viral nucleoside drugs. Likewise, transporter profiles and associated pharmacogenetics can be analyzed in patients which might assist in prediction of treatment outcomes. We have established that hCNT3 is highly selective for uridine over the other nucleosides in both Na^+- and Li^+-containing conditions; future studies can focus on uridine-hCNT3 binding characteristics to elucidate why this is the matter. Also, the transport mediated by other hCNT subtypes such as hCNT2 also deserve investigation because despite belonging to the same subfamily as hCNT1, it is inherently its own transporter. Additionally, a possible future direction of study could be to induce mutations in the cation binding sites to investigate their effects on cation mediated transport. Another future direction could be to conduct experiments with varying concentrations of nucleosides in the presence of Na^+, Li^+ or H^+ to elucidate the concentration-dependence of nucleoside transport by hCNT3.

5 | CONCLUSIONS

This study helps to further understand the cation-mediated nucleoside transport undertaken by hCNT1 and hCNT3. hCNT3 exhibits cation interactions with Na^+, H^+, and Li^+ that are not exhibited by other CNT proteins. Li^+ ions decrease the current generated by uridine uptake through hCNT1 and also through hCNT3 to a greater extent. Both hCNT1 and hCNT3 show a preference for Na^+ during uridine transport, as evidenced by the high maximal current generated under these conditions. On the other hand, these transporters exhibit the least preference for protons, given the low levels of current generated at all potentials tested. Relative to uridine, all other nucleosides elicited lower currents during their transport across hCNT3 in Li^+, indicating a structural basis for uridine supporting high levels of uptake through this transporter. Specifically, the presence of two functional groups on the nitrogenous base of nucleosides may provide more permissive coordination with nucleoside binding site, conferring more efficient transport, however further studies are required to validate these observations. Our study generated new knowledge in terms of hCNT3 substrate selectivity and voltage-dependence in the presence of Li^+ ions and the inhibitory effect of Li^+ ions on nucleoside uptake-induced currents.

ABBREVIATIONS

$CaCl_2$	Calcium chloride
ChCl	Choline chloride
CNTNW	Neisseria wadsworthii concentrative nucleoside transporter
CryoEM	Cryogenic electron microscopy
H^+	Hydrogen ion, proton
H_3O^+	Hydronium ion
hCNT	Human concentrative nucleoside transporter
hCNT1	Human concentrative nucleoside transporter 1
hCNT3	Human concentrative nucleoside transporter 3
hENT	Human equilibrative nucleoside transporter
I-V	Current-voltage relationship
KCl	Potassium chloride
Li^+	Lithium ion
LiCl	Lithium chloride
MBM	Modified Barth's medium
melB	Bacterial melibiose cotransporter
$MgCl_2$	Magnesium chloride
mM	Millimolar
mV	Millivolt
nA	Nanoamps
Na^+	Sodium ion
NaCl	Sodium chloride
NaDC-I	Sodium-dicarboxylate cotransporter
NT	Nucleoside transporter
PCMBS	p-chloromercuribenzene sulfonate
SCAM	Substituted cysteine accessibility method
SEM	Standard error of mean
SGLT	Sodium-dependent glucose cotransporter
TEVC	Two-electrode voltage clamp
vcCNT	Vibiro cholerae concentrative nucleoside transporter
Vcmd	Command voltage
Vh	Holding potential
Vm	Resting membrane potential

REFERENCES

Drew D, Boudker O. Shared Molecular Mechanisms of Membrane Transporters. Annual Review of Biochemistry 85: 543-572, 2016.

Gorraitz, E., M. Pastor-Anglada, and M.P. Lostao. 2010. Effects of Na^+ and H^+ ON steady-state and Presteady-state currents of the Human concentrative Nucleoside Transporter 3 (hCNT3). Pflügers Archiv - European Journal of Physiology. 460:617–632. doi:10.1007/s00424-010-0846-9.

Hirayama BA, Loo DDF, Wright EM. Cation Effects on Protein Conformation and Transport in the Na^+/Glucose Cotransporter. Journal of Biological Chemistry 272: 2110- 2115, 1997.

Hirschi M, Johnson ZL, Lee S-Y. Visualizing multistep elevator-like transitions of a nucleoside transporter. Nature 545: 66-70, 2017.

Johnson ZL, Cheong C-G, Lee S-Y. Crystal structure of a concentrative nucleoside transporter from Vibrio cholerae at 2.4 A. Nature 483: 489-493, 2012.

King, AE, Ackley MA, Cass CE, Young JD, Baldwin SA. Nucleoside transporters: from scavengers to novel therapeutic agents. Trends in Pharmacological Sciences 27: 416–425, 2006.

Mulinta R, Yao SYM, Ng AML, Cass CE, Young JD. Substituted cysteine accessibility method (SCAM) analysis of the transport domain of human concentrative nucleoside transporter 3 (hCNT3) and other family members reveals features of structural and functional importance. Journal of Biological Chemistry 292: 9505-9522, 2017.

Patejko M, Struck-Lewicka W, Siluk D, Waszczuk-Jankowska M, Markuszewski M. J. (2018). Chapter One – Urinary Nucleosides and Deoxynucleosides. Advances in Clinical Chemistry, 83:1-51. doi:10.1016/bs.acc.2017.10.001

Pajor AM, Hirayama BA, Loo DDF. Sodium and Lithium Interactions with the Na-/Dicarboxylate Cotransporter. Journal of Biological Chemistry 273: 18923-18929, 1998.

Smith, K. M., Ng, A. M., Yao, S. Y., Labedz, K. A., Knaus, E. E., Wiebe, L. I., … Young, J. D. (2004). Electrophysiological characterization of a recombinant human na+-coupled Nucleoside TRANSPORTER (hcnt1) Produced inxenopusoocytes. The Journal of Physiology, 558(3), 807-823. doi:10.1113/jphysiol.2004.068189

Smith KM, Slugoski MD, Cass CE, Baldwin SA, Karpinski E, Young JD. Cation coupling properties of human concentrative nucleoside transporters hCNT1, hCNT2 and hCNT3. Molecular Membrane Biology 24: 53-64, 2007.

Smith KM, Slugoski MD, Loewen SK, Ng AML, Yao SYM, Chen X-Z, Karpinski E, Cass CE, Baldwin SA, Young JD. The Broadly Selective Human Na Nucleoside Cotransporter (hCNT3) Exhibits Novel Cation-coupled Nucleoside Transport Characteristics. Journal of Biological Chemistry 280: 25436-25449, 2005.

Stecula A, Schlessinger A, Giacomini KM, Sall A. Human Concentrative Nucleoside Transporter 3 (hCNT3, SLC28A3) Forms a Cyclic Homotrimer. Biochemistry 56: 3475- 3483, 2017.

Yao SYM, Young JD. Inward- and outward-facing homology modeling of human concentrative nucleoside transporter 3 (hCNT3) predicts an elevator-type transport mechanism. Channels 12: 291-298, 2018,

Young JD, Yao SY, Baldwin JM, Cass CE, Baldwin SA. The human concentrative and equilibrative nucleoside transporter families, SLC28 and SLC29. Molecular Aspects of Medicine 34: 529-547, 2013.

Zhang J, Visser F, King KM, Baldwin SA, Young JD, Cass CE. The role of nucleoside transporters in cancer chemotherapy with nucleoside drugs. Cancer and Metastasis Reviews 26: 85–110, 2007.

Zhou Y, Liao L, Wang C, Li J, Chi P, Xiao Q, Liu Q, Guo L, Sun L, Deng D. Cryo-EM structure of the human concentrative nucleoside transporter CNT3. PLoS Biology 18: 1-14, 2020.

Zhu Q, Casey JR. Topology of transmembrane proteins by scanning cysteine accessibility mutagenesis methodology. Methods 41: 439-450, 2007.

How to cite this article:

Kanagala, D. (2022). Characterizing Lithium-Mediated Nucleoside Transport by Human Concentrative Nucleoside Transporters 1 and 3 (hCNT1 and hCNT3). *Eureka.* 7(1). https://doi.org/10.29173/eureka28774